Density Functional Theory Study of the Conformational Space of Phenyl Benzoate, a Common Fragment in Many Mesogenic Molecules

Giorgio Cinacchi* and Giacomo Prampolini‡

Dipartimento di Chimica, Università di Pisa, Via Risorgimento 35, I-56126 Pisa, Italy

Received: January 7, 2005; In Final Form: May 16, 2005

The complete conformational space of phenyl benzoate (three coupled rotors) has been studied by B3LYP density functional theory (DFT) at the 6-31+G* basis set level. The overall quality of the DFT results has been checked via Möller−Plesset second-order perturbation theory (MP2) calculations performed on a few significant molecular geometries. Contrary to the general belief, we have found that rotation around the C(═O)−O bond is not more restricted than rotation around the C(═O)−C bond. We have commented on the location and magnitude of the molecular dipole moment and their dependence on conformation. The energy data have been fitted through an expression containing a Fourier expansion plus a Lennard-Jones term, suitable to be used in computer simulations or to assist analysis of experimental data.

1. Introduction

Phenyl benzoate (PB) occurs as a building block in many molecules giving rise to systems of fundamental and practical interest. For example, chiral smectic C and banana liquid crystal-forming molecules[1,2] often have PB as a fragment of their molecular architectures. Therefore, a detailed knowledge of the conformational space of PB may help to comprehend structure−properties relationships in complex systems such as those aforementioned.

As shown in Figure 1, PB conformation is mainly defined by three dihedral angles: φ_1, which describes the rotation of the phenyl ring "a" around the C−O bond; φ_2, which describes the rotation of the phenyl ring "b" around the C(═O)−C bond; and φ_3, which describes the rotation around the C(═O)−O bond. The structure of PB has been the subject of a number of studies, both experimental and theoretical. X-ray diffraction experiments[3,4] indicate that, in the crystalline phase, PB exists in one conformation, defined by $\varphi_1 \approx 70°$, $\varphi_2 \approx 10°$, and $\varphi_3 = 180°$.

In a fluid phase, however, a molecule is expected to explore a continuous range of conformations. NMR spectroscopy in nematic liquid crystal solvents (LX-NMR) is the technique of choice to experimentally study the structure of molecules in condensed fluid phases.[5] This technique was applied to PB, and the proton dipolar coupling data, analyzed via the additive potential (AP) mean field model,[6] were found to be consistent with a minimum energy conformation in which $\varphi_1 \approx 50°$, $\varphi_2 = 0°$, and $\varphi_3 = 180°$. The structure of PB in the dilute fluid phase was then investigated by gas electron diffraction (GED).[7] The analysis of the GED data, supported by ab initio calculations, showed that the conformation of minimum energy is $\varphi_1 = 64(-12, +26)°$, $\varphi_2 \approx 0°$, and $\varphi_3 = 180°$. This result was later confirmed by the detailed quantum chemical study of ref 8. In that work, the authors investigated the structure and conformations of PB by the Hartree−Fock (HF) method, Möller−Plesset second-order perturbation theory (MP2), and density functional theory (DFT) with several polarized basis sets. In particular, they obtained the best agreement with the X-ray or GED experimental measures by computing the PB minimum energy conformation using diffuse functions with the B3PW91 and the B3LYP DFT functionals.

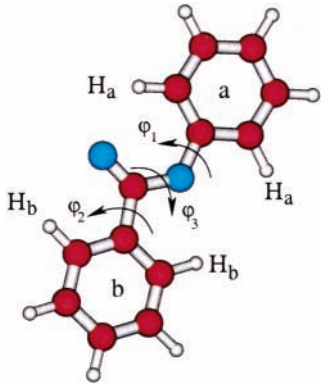

Figure 1. Phenyl benzoate. The values of the dihedral angles are defined such that this conformation corresponds to $\varphi_1 = 0°$, $\varphi_2 = 0°$, and $\varphi_3 = 180°$. Note that in most of the previous works, φ_3 was defined as zero in the illustrated molecular geometry.

In both refs 7 and 8 it was assumed that the rotation around the C(═O)−O bond is so rigid that the PB molecule should always exist in conformations with the dihedral angle φ_3 fixed to 180°, thus considerably reducing the complexity of PB conformational space from three (generally coupled) rotors to two (essentially independent) rotors. In both of these works, analytical expressions were provided for the conformational energy dependence on the two investigated dihedrals. However, there is evidence from the LX-NMR study[6] that this apparently plausible assumption may not be correct. In fact, the distribution in φ_3 was found to be fairly large, and the rotation around the C(═O)−C bond was found to be more hindered than that around C(═O)−O, so that the probability distribution $P(\varphi_1, \varphi_2, \varphi_3)$ is well-approximated by $P(\varphi_1, 0, \varphi_3)$.

Unfortunately, definite and precise conclusions about the shape of the conformational space of flexible molecules cannot be drawn from an NMR study alone, both because of the dependence on the orientational order of the measured quantities (e.g., dipolar couplings) and because it is difficult to exhaustively

* Corresponding author. E-mail: g.cinacchi@sns.it.
‡ E-mail: giacomo@dcci.unipi.it.

10.1021/jp050102h CCC: $30.25
Published on Web 06/23/2005

model flexibility, not to mention possible non-negligible solvent effects. Nevertheless, LX-NMR spectroscopy is a very valuable source of qualitative results, in that it might reveal particular features in conformational space that call for further and more refined quantum chemical computations.[9] Conversely, an effective way to address the problem of the orientation and conformation of a solute in nematic solvents could be to supplement the analysis of the experimental data with a separate conformational analysis undertaken by quantum chemical methods on the isolated molecule.[10]

With this in mind, we have decided to perform a DFT study of the whole conformational space of PB. Thus, following the LX-NMR results, we have gone beyond the assumption that φ_3 is fixed at 180°, and we have treated PB as a three-coupled rotor system. The energy data, calculated at the 6-31+G* level, have been fitted to an analytical function suitable to supplement experimental data analysis or to be used in atomistic computer simulations. The latter has emerged in the past decades as a very important tool to study the behavior of complex systems such as liquid crystals and polymers. For example, refs 11, 12, and 13 contain computer simulation studies on systems of mesogenic molecules having PB fragments in their cores. In particular, our calculations might be of help in the theoretical[14,15] and experimental[16,17] studies of the novel banana liquid crystal molecules.

Our paper is arranged as follows: in the next section we provide computational details of our calculations, and the results are presented and discussed in section III; finally, our conclusions are presented in section IV.

2. Computational Details

In all calculations with the density functional B3LYP method,[18] a diffuse and polarized double-ζ 6-31+G* basis set was employed. This choice was motivated by the results presented in ref 8, in which it was found that the aforementioned method provides the best agreement with the experimental GED data. Moreover, to further validate this choice, supplementary calculations at the MP2 level with the same and a larger (6-31+G**) basis set have been undertaken on a few paradigmatic conformations.

During all geometry optimizations, no symmetry restriction was imposed except the torsional angles defined in Figure 1. In all cases, the absolute energy minimum was obtained by a complete geometry optimization. At the DFT level, a grid of 175 points was constructed by varying φ_1, φ_2, and φ_3 in the 0−180° range, in steps of 30°, 45°, and 45°, respectively. All calculations[19] were performed with the GAUSSIAN 03 package.[20]

The resulting DFT energy surface versus the torsional dihedrals was then represented by a suitable expansion onto trigonometric functions. Moreover, to improve the performance of the fitting procedure, the Fourier expansion was coupled to an intramolecular Lennard-Jones function between the inner aromatic hydrogen atoms H_a and H_b (see Figure 1). Thus, the fitting function $F(\varphi_1, \varphi_2, \varphi_3)$ can be written as

$$F(\varphi_1,\varphi_2,\varphi_3) = \sum_{k=0}^{N_1} a_k \cos(2k\varphi_1) + \sum_{k=0}^{N_2} b_k \cos(2k\varphi_2) + \sum_{k=0}^{N_3} c_k \cos(k\varphi_3) + G(\varphi_1,\varphi_2,\varphi_3) \quad (1)$$

with N_j ($j = 1, 2, 3$) the number of the cosine terms for angle j and

$$G(\varphi_1,\varphi_2,\varphi_3) = \sum_{i=1}^{N_H} 4\epsilon\left[\left(\frac{\sigma}{r_i(\varphi_1,\varphi_2,\varphi_3)}\right)^{12} - \left(\frac{\sigma}{r_i(\varphi_1,\varphi_2,\varphi_3)}\right)^{6}\right] \quad (2)$$

in which N_H is the number of pairs of interacting hydrogen atoms and r_i is the distance between the H atoms of the ith couple. The ensemble of the least-squares fitting parameters is thus composed by [a,b,c,ϵ,σ].

The choice of the coupling function $G(\varphi_1,\varphi_2,\varphi_3)$ was prompted by the need for a compromise between the accuracy of the fitting process and the simplicity of the fitting expression. The most natural way to account for the rotor coupling would be to consider a full Fourier expansion with cross terms [e.g., $\cos(\varphi_i)\cos(\varphi_j)$ or $\cos(\varphi_k)\sin(\varphi_l)$]. Nevertheless, we have chosen eq 2 because in most of the common force fields (e.g., AMBER,[21] CHARMM,[22] GROMOS[23]) this is the standard form already implemented for nonbonded intramolecular interactions.

3. Results and Discussion

3.1. DFT and MP2 Comparison. Although DFT methods are generally known to perform well in torsional barrier computations for a number of organic molecules (see, for instance, refs 9, 24−28), they cannot be confidently extended a priori to a given molecular system. In this respect, ab initio post-self-consistent field (post-SCF) methods would offer a more reliable tool, provided that sufficiently large basis sets are employed. To verify the reliability of our DFT calculations, MP2 benchmarks have been performed on a few significant conformations. Specifically, the minimum energy geometry and the four conformations specified by the triplets [$\varphi_1 = 0°$, $\varphi_2 = 0°$, $\varphi_3 = 180°$], [$\varphi_1 = 90°$, $\varphi_2 = 0°$, $\varphi_3 = 180°$], [$\varphi_1 = 60°$, $\varphi_2 = 45°$, $\varphi_3 = 180°$], [$\varphi_1 = 60°$, $\varphi_2 = 0°$, $\varphi_3 = 135°$] have been computed at the MP2 level of theory, with both 6-31+G* and 6-31+G** basis sets. The value of φ_1 in the fully optimized geometry, together with the torsional energy barriers of the four abovementioned conformations (ΔE^0, ΔE^1, ΔE^2, and ΔE^3, respectively), is reported in Table 1. In the same table, the latter quantities are compared with the corresponding DFT values and the available GED experimental data.[7]

DFT and MP2 methods yield a minimum energy conformation consistent with that deduced from the experiment reported in ref 7. In particular, the value of the most flexible dihedral φ_1 is found by both theoretical methods in the experimental range [64(−12, +26)°]. This wide interval, as well as the relatively low experimental value of ΔE^1, suggests that the potential curve of the rotation about φ_1 is rather flat in its minimum region, as confirmed by the computed ΔE^1 values. Conversely, regarding the other torsional barriers, differences arise in employing different methods; overall, the DFT barriers are more similar to the experimental ones. It is of interest to observe that the trend in the MP2 computed barriers appears to converge toward the DFT values as the dimensions of the basis set are increased. This fact has already been observed in other molecular systems.[24,26,27]

However, if a large number of geometries has to be computed, to efficiently sample a complex, three-rotor conformational space, MP2 methods are ruled out by the computational cost (see last column of Table 1) required to handle a sufficiently large basis set. For this reason, the DFT method with the 6-31+G* basis set has been employed to achieve this goal.

3.2. DFT Conformational Space. The minimum energy conformation ($\varphi_1 \simeq 60°$, $\varphi_2 \simeq 0°$, and $\varphi_3 \simeq 180°$) is within the reported error of GED measurements[7] [64(−12, +26)°, 0°, 180°]

TABLE 1: DFT, MP2, and Corresponding Experimental Results[a]

method	basis set	φ_1^0	ΔE^0	ΔE^1	ΔE^2	ΔE^3	t^0
DFT	631+G*	61	3.15	0.29	10.67	18.31	10
MP2	631+G*	71	12.52	0.57	6.75	19.57	45
MP2	631+G**	71	9.53	0.29	8.58	19.27	285
expt		64	5.02	0.13	8.37		

[a] Results are for the following quantities: φ_1 optimized value in degrees (φ_1^0); energy barrier heights in kJ/mol (ΔE^0, ΔE^1, ΔE^2, ΔE^3; definitions of which are given in the text); and central processing unit (CPU) time in hours (t^0) requested on a 2.6 GHz Pentium IV processor for a full optimization.

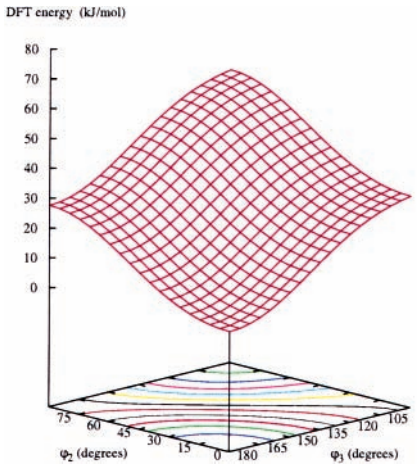

Figure 2. PB two-dimensional torsional energy surface, as obtained from the fitted analytical expression (see eq 1 and Table 2). The φ_2 and φ_3 dihedrals are varied, whereas φ_1 is kept fixed at 60°. In the $\varphi_2-\varphi_3$ plane, surface contours are drawn in increments of 5 kJ/mol.

and also in fair agreement with NMR results[6] (50°, 0°, 180°). In the latter work, the authors state that the conformations are distributed over a range of all three dihedral angles, in contrast with the assumptions of refs 7 and 8, which constrain the C═O bond as being cis to the O−C_6H_5 one (i.e., $\varphi_3 = 180°$), thus reducing the PB molecule to a two-decoupled rotor system.

Our computed data partly support the LX-NMR conclusions. The two-dimensional plot of the PB torsional energy surface, obtained by varying dihedrals φ_2 and φ_3 and fixing φ_1 at 60°, is reported in Figure 2. It can be seen that variations of φ_2 or φ_3, with respect to their minimum energy values, result in a similar energy increase, the respective surface gradient being of comparable magnitude. Despite the strong dependence of the torsional energy on φ_2 and φ_3, small distortions from their equilibrium values cannot be excluded at normal temperatures.

Indeed, as can be seen from Figure 3, the energy barrier for a 45° rotation of φ_3 from its minimum value (being $\varphi_1 = 60°$ and $\varphi_2 = 0°$) amounts to ≃18 kJ/mol (see panel b), which is not too far from the value of ≃13 kJ/mol obtained for the same rotation performed on φ_2 and reported in panel a.

In addition, it is worth noticing that the libration around φ_3 is accompanied by a significant variation of both the magnitude and the orientation of the molecular dipole moment (see Figure 3d,f). Conversely, it is evident from Figure 3c,e that the latter is almost constant (≃2 D) and aligned along the C═O bond direction when φ_2 is varied.

In the lower panel of Figure 4, the torsional potential dependence on φ_1 with $\varphi_2 = 0°$ and $\varphi_3 = 180°$ is reported and compared with literature results. The overall shape of the potential curve is qualitatively in accord with all the reported sets. However, major differences were found in the barrier

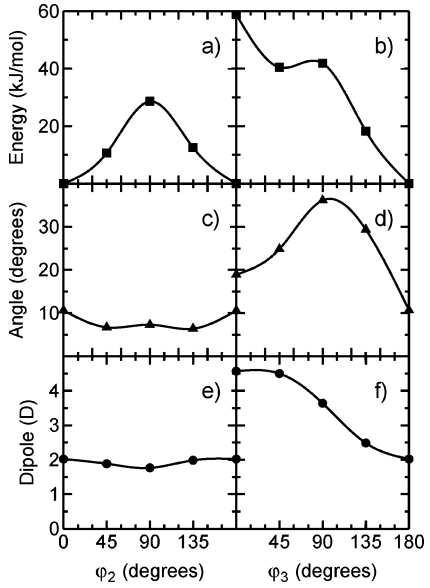

Figure 3. φ_2 and φ_3 dependence of the following computed quantities: (a,b) torsional energy; (c,d) angle between the C═O bond and the molecular dipole moment; (e,f) molecular dipole moment. All values refer to $\varphi_1 = 60°$; in panels (a), (c), and (e), $\varphi_3 = 180°$; in panels (b), (d) and (f), φ_2 is fixed at 0°.

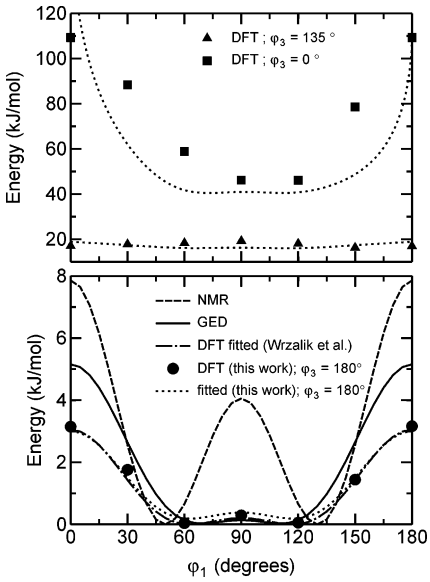

Figure 4. Torsional energy vs φ_1 curves at different values of φ_3 and $\varphi_2 = 0°$. In the upper panel, the $\varphi_3 = 135$ and 0° energy DFT data (symbols) are reported together with the corresponding fitted curves (dotted lines). In the lower panel, the computed energies at $\varphi_3 = 180°$ are compared with existing experimental (NMR, dashed; GED, solid) and theoretical data (fitted functions for ref 8, dot−dashed; this work, dotted).

heights. GED experiments[7] seem to indicate a homogeneous distribution population in the approximate range of 60−120°, the 90° barrier being extremely small. Nevertheless, it must be noted that such measurements heavily rely on the RHF//6-31G** computed quantities used in the experimental data analysis and on the neglect of the flexibility around φ_3. This flatness does not appear from the NMR[6] results; in contrast, the 90° conformer stands out clearly as a transition state. In their work, Wrzalik et al.[8] were able to reproduce the GED findings through a comprehensive quantum chemical study, giving an analytical expression for the two-dimensional PB conformational space. Their results coincide with ours for the particular cases of a

TABLE 2: Fitting Parameters for $N_1 = N_2 = 3$ and $N_3 = 4$[a]

k	a_k	b_k	c_k
0	13.84	6.90	18.70
1	1.31	−13.66	16.92
2	0.57	0.78	−5.18
3			3.35
ϵ		1.25×10^{-4}	
σ		5.55	

[a] All Fourier coefficients are reported in kJ/mol. ϵ and σ are in kJ/mol and Å, respectively.

variable φ_1 with φ_2 and φ_3 fixed at the same values of the minimum energy conformation.

It seems that one can state with confidence that the conformational potential of PB is smooth with respect to variations of φ_1, whereas the molecule librates around $\varphi_2 = 0°$ and $\varphi_3 = 180°$. Furthermore, considering $\varphi_3 \neq 180°$ also reveals the existing coupling between the three rotors. Indeed, the shape of the φ_1 curves, shown in the upper panel of Figure 3, is strongly dependent on the φ_3 values.

The DFT-computed energies have been fitted to an analytical expression in which we have added to Fourier terms the intramolecular Lennard-Jones term between a pair of ortho hydrogens H_a and H_b (see Figure 1), that is, $N_H = 4$ in eq 1. This permits us to take into account the correlation among the dihedrals, which is augmented by lowering φ_3. The corresponding fitting curves are reported in Figure 4 with dotted lines, and the fitting parameters are given in Table 2. In consideration of the high energies found for φ_3 values less than 135°, which rule out the existence of such conformations at normal temperatures, we have preferred to bias the fitting toward the best reproduction of a lower energy region. For this reason the standard deviations were computed separately for different energy ranges, namely, 0−25, 25−50, and >50 kJ/mol, giving 4.8, 6.1, and 16.9 kJ/mol, respectively. By looking at the overall deviation (11.6 kJ/mol), one can see that the major contribution to the inaccuracy of the fit comes from the error in reproducing high energy values (see also the $\varphi_3 = 0°$ curve in Figure 4).

4. Conclusions

The entire conformational space of PB has been mapped by calculating, through the B3LYP density functional method at the 6-31+G* basis set level, the energy of a number of molecular geometries generated by varying the three dihedral angles defining a conformation. The computed data, benchmarked with MP2 calculations on selected molecular geometries, show good accord with previous experimental and theoretical results, wherever comparison is possible. Moreover, and contrary to previous theoretical works, the energy dependence on the middle rotator (φ_3) was also considered, as suggested by the LX-NMR results. The inclusion of the φ_3 energy dependence forces one to consider the correlation among the dihedrals in an analytical expression suitable for atomistic computer simulations and for supplementing experimental data. This has been done by adding Lennard-Jones intramolecular terms to a standard Fourier expansion. The motion of PB in its conformational space is characterized by a rather free rotation around the C_6H_5−O bond (φ_1), together with a libration around the values of $\varphi_2 = 0°$ and $\varphi_3 = 180°$. The latter, despite being small in amplitude, is far from being unimportant because it is associated with a significant variation of direction and magnitude of the molecular dipole moment. Taking into account the dipole moment dependence on the overall PB conformations may be crucial if one aims to reproduce the behavior and properties of soft materials that have PB as a constitutive fragment.

Supporting Information Available: Table of computed DFT (B3LYP/6-31+G*) torsional relative energies for phenyl benzoate. This material is available free of charge via the Internet at http://pubs.acs.org.

References and Notes

(1) Collings, P. J.; Hird, M. *Introduction to Liquid Crystals*; Taylor and Francis: London 1997.
(2) Pelzl, G.; Diele, S.; Weissflog, W. *Adv. Mater.* **1999**, *11*, 707.
(3) Adams, J. M.; Morsi, S. E. *Acta Crystallogr.* **1976**, *B32*, 1345.
(4) Shibakami, M.; Sekiya, A. *Acta Crystallogr.* **1995**, *C51*, 326.
(5) *NMR of Ordered Liquids*; Burnell, E. E., de Lange, C. A., Eds.; Kluwer: Dordrecht, The Netherlands, 2003.
(6) Emsley, J. W.; Furby, M. I. C.; De Luca, G. *Liq. Cryst.* **1996**, *21*, 877.
(7) Tsuji, T.; Takeuchi, H.; Egawa, T.; Konaka, S. *J. Am. Chem. Soc.* **2001**, *123*, 6381.
(8) Wrzalik, R.; Merkel, K.; Kocot, A. *J. Mol. Model.* **2003**, *9*, 248.
(9) Cinacchi, G.; Prampolini, G. *J. Phys. Chem. A* **2003**, *107*, 5228.
(10) Cinacchi, G.; Veracini, C. A. The Maximum Entropy Principle in the Treatment of Structural Data from Liquid Crystal NMR Spectroscopy, In *Universality and Diversity in Science: Festschrift in Honor of Naseem K. Rahman's 60th Birthday*; World Scientific: Singapore, 2004.
(11) Jung, B.; Schurmann, B. L. *Mol. Cryst. Liq. Cryst.* **1990**, *185*, 141.
(12) Huth, J.; Mosell, T.; Nicklas, K.; Sariban, A.; Brickmann, J. *J. Phys. Chem.* **1994**, *98*, 7685.
(13) Jang, W. G.; Glaser, M. A.; Park, C. S.; Kim, K. H.; Lansac, Y.; Clark, N. A. *Phys. Rev. E* **2001**, *64*, 051712.
(14) Imase, T.; Kawauchi, S.; Watanabe, J. *J. Mol. Struct.* **2001**, *560*, 275.
(15) Cacelli, I.; Prampolini, G. *Chem. Phys.* **2005**, *314*, 283.
(16) Jàkli, A.; Huang, Y.; Fodor-Csorba, K.; Vayda, A.; Galli, G.; Diele, S.; Pelzl, G. *Adv. Mater.* **2003**, *15*, 1606.
(17) Niwano, H.; Nakata, M.; Thisayukta, J.; Link, D.; Takezoe, H.; Watanabe, J. *J. Phys. Chem. B* **2004**, *108*, 14889.
(18) Becke, A. D. *J. Chem. Phys.* **1993**, *98*, 5648.
(19) The DFT energy data are given as Supporting Information; all molecular geometries are available from the authors upon request.
(20) Frisch, M. J., et al. *Gaussian 03*; Gaussian, Inc.: Pittsburgh, PA, 2003.
(21) Wiener, S. J.; Kollmann, P. A.; Nguyen, D. T.; Case D. A. *J. Comput. Chem.* **1986**, *7*, 230.
(22) Brooks, B. R.; Bruccoleri, R. E.; Olafson, B. D.; States, D. J.; Swaminanthan, S.; Karplus, M. *J. Comput. Chem.* **1983**, *4*, 187.
(23) Hermans, J.; Berendsen, H. J. C.; van Gusteren, W. F.; Postma, J. P. V. *Biopolymers* **1984**, *23*, 1.
(24) Tsuzuki, S.; Uchimaru, T.; Tanabe, K. *Chem. Phys. Lett.* **1995**, *246*, 9.
(25) Göller, A.; Grummt, U. W. *Chem. Phys. Lett.* **2000**, *321*, 399.
(26) Klocker, J.; Karpfen, A.; Wolschann, P. *Chem. Phys. Lett.* **2003**, *377*, 566.
(27) Raos, G.; Famulari, A.; Marcon, V. *Chem. Phys. Lett.* **2003**, *379*, 364.
(28) Cacelli, I.; Prampolini, G. *J. Phys. Chem. A* **2003**, *107*, 8665